

We are IntechOpen, the world's leading publisher of Open Access books Built by scientists, for scientists

6,900

Open access books available

186,000

International authors and editors

200M

Downloads

Our authors are among the

154

Countries delivered to

TOP 1%

most cited scientists

12.2%

Contributors from top 500 universities



WEB OF SCIENCE™

Selection of our books indexed in the Book Citation Index
in Web of Science™ Core Collection (BKCI)

Interested in publishing with us?
Contact book.department@intechopen.com

Numbers displayed above are based on latest data collected.
For more information visit www.intechopen.com



Numerical Simulation of Fission Product Behavior Inside the Reactor Containment Building Using MATLAB

Khurram Mehboob and
Mohammad Subian Aljohani

Additional information is available at the end of the chapter

<http://dx.doi.org/10.5772/intechopen.70706>

Abstract

The aim of this work is to carry out the numerical simulation of fission product (FP) behavior inside the reactor building under loss of coolant accident (LOCA) using MATLAB. For this purpose, a kinetic model has been developed and implemented in MATLAB to study the behavior of in-containment FPs during postulated LOCA for typical 1000 MW pressurized water reactor (PWR). A continuous release of the FPs from the reactor pressure vessel (RPV) has been implemented with coolant retention. The in-containment FP behavior is influenced by containment atmosphere and containment safety systems. The sensitivity analysis and removal rate of airborne isotopes with the containment spray system have been studied for various spray activation time, spray failure time, droplet size and spray pH value. The droplet size and pH value of the spray system effectively remove the airborne isotopes. The alkaline (sodium thiosulfate, $\text{Na}_2\text{S}_2\text{O}_3$) spray solution and spray with pH 9.5 have similar scrubbing properties for iodine. However, the removal rate from the containment spray system has been found an approximately inverse square of droplet diameter ($1/d^2$).

Keywords: PWR, fission products, MATLAB, sodium thiosulfate, droplet diameter

1. Introduction

The nuclear reactor systems are sufficiently complex that there could be the possibility of an accident followed by the release of fission product (FPs). Such a release could require multiple failures of safety systems and barriers. In the case of a break in the hot/cold leg in a pressurized water reactor (PWR), coolant and energies are first released from the reactor coolant system to the containment through the break. The FP also released along with the coolant. This type of accident usually occurs in the high-pressure cold leg. The worst

condition of such an uncontrolled break is the guillotine type of break. In such type of accident, the envelope of primary systems is breached [1]. If such an accident is not controlled by safety systems, then such accidents may transform into the severe accident.

In severe accidents, FP is released during the progression of accidents [2]. Owing to the strong influence of thermal hydraulics on FP release and transportation, FP release and transport mechanism is very complicated and complex. The FP behavior inside the containment is the fundamental of the source term. The source term results are the outputs of level 2 PSA [3], which are necessary for radiological assessments and consequences. The dominant FPs that constitute in hazardous effects can be categorized as noble gasses (Xe, Kr), volatile (I, Cs, Te), semi-volatile (Ru, Ag, Ba, Sr, Tc, Rh) and nonvolatile (Nb, Zr, Y, Pd, La, Mo, Tc, Nd, Ce) ([4, 5]). The aerosols are ^{129}Te , ^{127}Te , ^{105}Rh , ^{103}Ru , ^{105}Ru , ^{137}Cs , ^{138}Cs , ^{89}Sr , ^{90}Sr and ^{140}Ba . These isotopes release in the particulate form, and going through agglomeration and nucleation process, they form aerosols [6]. However, iodine may transform into volatile species and possess a complex chemistry [7]. The common organic form of iodine is available in chemical forms as CH_3I , CsI and HI [8]. The behavior of FP is highly influenced by the in-containment atmosphere, heat loads, containment pressure and steam generation rate. The containment is installed with the spray system and cooling fans to prevent the early over-pressurization due to the heat load. The containment spray system is significant in enhancing the early depletion of radionuclides during early in-vessel release phase from the containment atmosphere. The spray system is automatically activated, as an emergency designed device to prevent containment integrity [9].

The FP release from a nuclear power plant (NPP) is known as a key factor affecting both the design of safety equipment and safety evaluation, including safety and risk assessment [10]. Experimental research on FP release behavior was conducted by many investigators [11–13]. Many experiments had played a significant role in understanding the behavior of aerosols, FPs, iodine chemistry, and transportation under accident situations [13–17]. The Phébus-FP project [18] was the most impressive program initiated to study the behavior of FP. The main objectives of this project were (1) to minimize the uncertainty in source term evaluation, (2) to study the FPs, structural and control rod material release transportation and deposition from the degraded core through coolant, and (3) and behavior of FP inside the containment building [19, 20]. Meanwhile, several analytical and computational codes were developed. ASTEC is one of the most popular codes used to study the behavior of FPs in severe accident conditions [21]. MELCOR along with MACCS can be used to assess FP release and assessment of radiological consequence [22]. MAAP is the most popular tool to calculate severe accident source term, and its quick calculation is its prime character. Therefore, MAAP code is widely used in the nuclear industry [23].

Moreover, the numerical simulation of FP activity has been carried out by several researchers. [24] have developed an analytical model FIPRAP “FP Release Analysis Program” for the numerical simulation of FPs released from the fuel. The FIPRAP code can estimate the volatile FPs released from the nuclear fuel under changing irradiation conditions with the incorporation of all physical phenomena and fulfill the requirements of fuel designing, performance, degradation and source term estimation codes. Lewis et al. [25] have presented a review of FPs release modeling in support of fuel failure monitoring analysis for the characterization and allocation of defected fuel. A generalized model for FP transport in the fuel-to-sheath gap was

given by [26]. Koo et al. [27] have proposed a model describing pallet oxidation and bubble formation at grain boundaries, their interlinkages, and release into exposed surfaces. Avano [28] described a good model for the description release of FPs from the porous ceramic fuel, its leakage from cladding and mixing with the primary coolant. Tucker and white [29] have proposed an analytical model for the estimation of FPs from ceramic UO₂ fuel. In this model, the PF leakage probabilities from the fuel interior through grain are figured out. These probabilities strongly depend on the interconnectivity of pores in the ceramic fuel. Awan et al. [30] have also carried out the numerical simulation of FP activity in the reactor primary coolant. The proposed developed model is hybrid and analyzes the static and dynamic FP activity in the primary coolant of the reactor [31].

The goal of this chapter is to carry out the numerical simulation of FP behavior inside the reactor containment building under LOCA using MATLAB. The calculation process of iodine and other FPs is shown in **Figure 1**. A semi-kinetic model has been developed and implemented in MATLAB to carry out the sensitivity analysis of FPs during postulated LOCA for typical 1000 MW PWR. The kinetic model is presented in section II, which contains the deterministic as well as the kinetic approach. The deterministic computational methodology and computational steps flow chart are described in Section III. Next, the flow chart of model and implementation of model in MATLAB are described in Section IV. The examples and outcomes of the simulation results are presented in Section V. Finally, Section VI is the conclusion.

2. In-containment fission product release model

Figure 1 shows the process of release of FPs from fuel to cladding, cladding to coolant and then to the containment. In this work, a 1000-MW pressurized water reactor (PWR) has been considered with the design specification as shown in **Table 1**. The PWR system along with the containment system is shown in **Figure 2**. We have developed a real-time kinetic model to simulate the FP behavior inside the containment. The analytical model is a set of coupled ordinary differential equations (ODEs). The FP activity inside the reactor containment building and on the surfaces and walls of the containment is governed by the following sets of ODEs [8, 32, 33].

$$\frac{dm_{v,i}(t)}{dt} = -\lambda_i m_{v,i}(t) - u_{t,i} \frac{S}{V} m_{v,i}(t) - \alpha \frac{F}{V} m_{v,i}(t) - R_{res,i} \frac{\eta_{rc}}{V} m_{v,i}(t) - \frac{L_r}{V} m_{v,i}(t) + r_i \frac{S}{V} m_{s,i}(t) + P_i(t) \quad (1)$$

where

$$\alpha = \begin{cases} H\eta_i & \text{Iodine} \\ \frac{3hEa}{2d} & \text{other FPs} \end{cases} \quad (2)$$

$$\frac{dm_s(t)}{dt} = v_t m_v(t) - r m_s(t) \quad (3)$$

where *i* indicates the isotope, whereas *V* and *S* indicate the volumetric and surface activities of *i*th isotope. The puff release of FP is $m_v(t) = f_x \times f_f \times f_p \times f_c \times A_c/V \text{ g.m}^{-3}$. The values of various parameters used in these simulations are listed in **Table 2**.

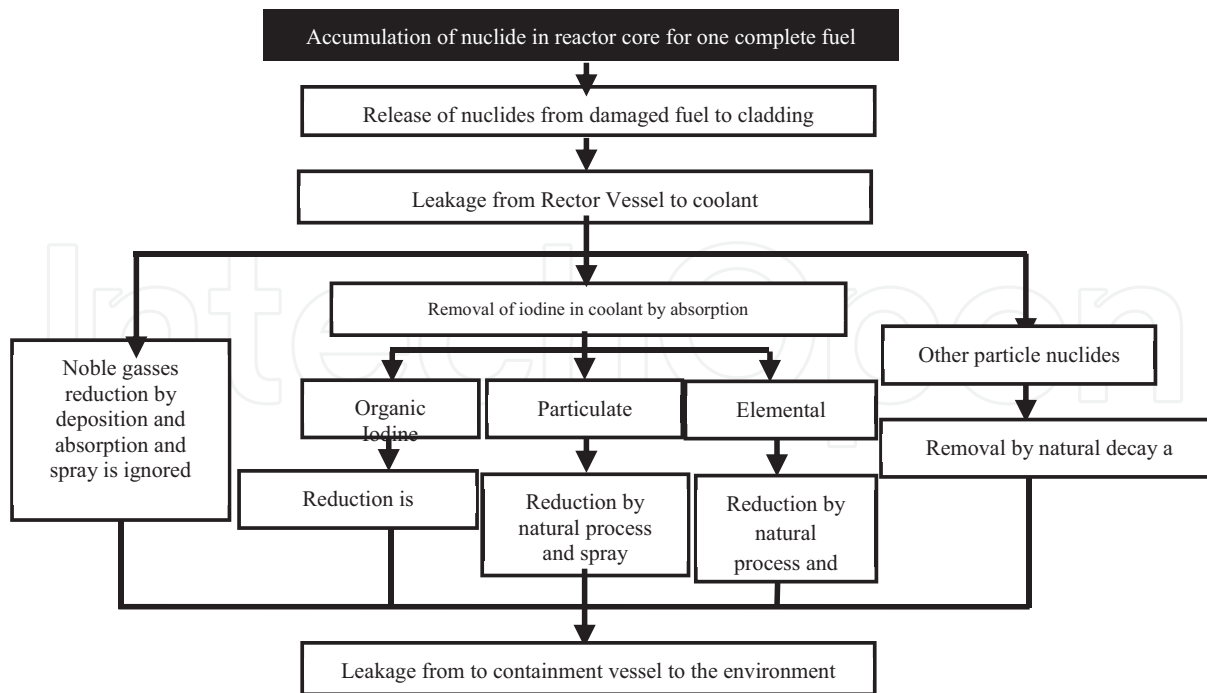


Figure 1. The calculation process of the FP behavior inside the reactor building.

Parameters	Value
Reactor	PWR
Fuel type	UO ₂
Average fuel enrichment wt%	2.4%
Specific power (MWth/kg U)	33.3
Power density (MWth/m ³)	66.6
System pressure (MPa)	15.166
System pressure (MPa)	14.96
Coolant flow (kg/s)	17387.7
Core height (m)	12.41
Core active region (m)	3.65
Core diameter (m ²)	3.81
Fuel assemblies	177
Control rod assemblies	69
Cladding material	Zircaloy
Fuel rod outer diameter (cm)	1.092
Rod pitch (cm)	1.443
Fuel assembly matrix	15 × 15
Coolant inlet temperature (k)	564.81

Parameters	Value
Coolant outlet temperature (k)	592.98
Control rods	1104
Control rod material	Ag (80%)-In (15%)-Cd (5%)

Table 1. Design parameters of typical 1000 MW reactor [34, 35].

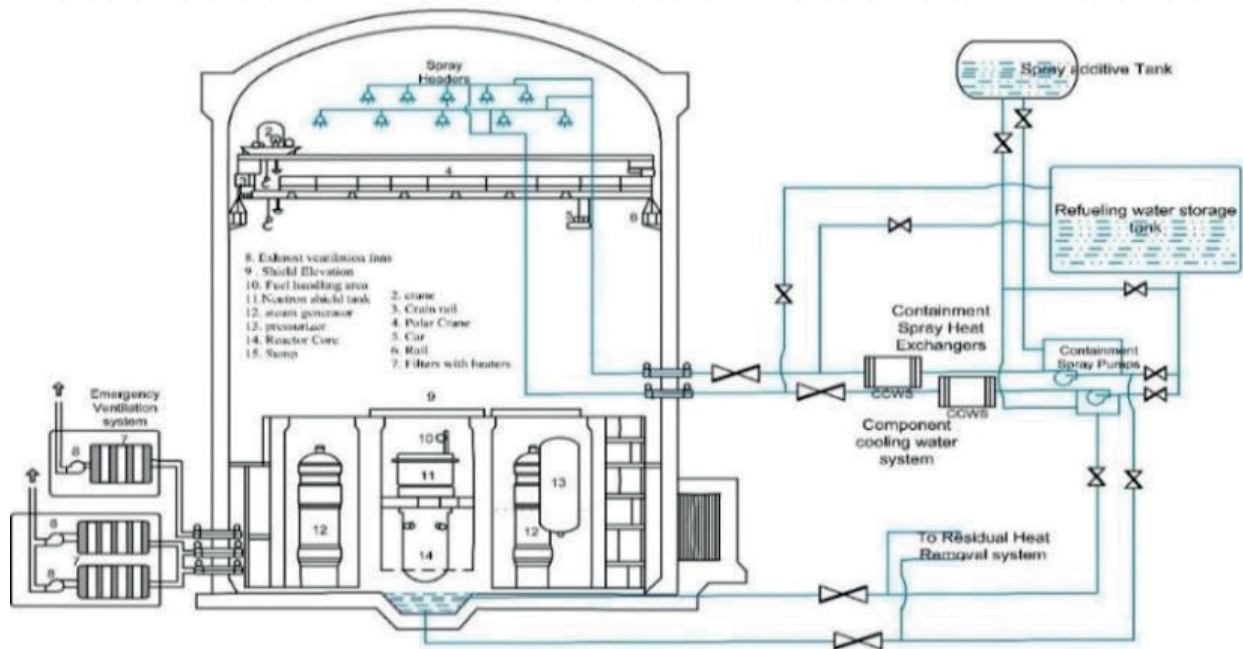


Figure 2. A schematic diagram of a typical PWR system with the containment spray system.

Parameters	Symbol	Value
Containment free volume	V (m^3)	57,600
Containment free surface	S (m^2)	~34,374
Leakage rate	L_r (m^3/s)	14.15
Core damage fraction	f_c (%)	35%
Fuel release fraction	f_f (%)	9.0×10^{-1}
Water release fraction	f_p (%)	3.00×10^{-1} – 1.0×10^2
Recirculation rate	R_{res} (m^3/s)	1–5
Recirculation filtration efficiency	η_{res} (%)	10–90%
Exhaust filter efficiency	η_{ex} (%)	90–98
Fraction of immediately released radioisotopes	f_x (%)	2.0×10^{-1}
Mixing rate	w_x (s^{-1})	0.1–1.0
Spray flow rate	F (m^3/s)	0.1–1.0

Parameters	Symbol	Value
Droplet size	d (micron)	100–1000
Deposition velocity (ud)	(m/s)	5.5×10^{-4}
Resuspension rate	s^{-1}	$\leq 2.3 \times 10^{-6}$

Table 2. Important parameters used for simulation [36].

2.1. Kinetic source of fission product

The last term in Eq. (1) is the source of FP from the reactor pressure vessel. The kinetic source is modeled as [37].

$$P(t) = (1 - f_x) A_c f_f f_p f_c \frac{K}{V} e^{(-w_x t)} \quad (4)$$

$$K = \frac{w_x \times (w_x / T)}{w_x - w_x / T} \quad (5)$$

The $(1 - f_x) \exp.(-w_x t)$ is the airborne FP activity released along with the coolant with mixing rate w_x . Where K is the normalization constant and expressed as follows. The overall radioactive mass inventory, including kinetic and static parts, is depicted in Eq. (6).

$$A_c = f_x A_c + (1 - f_x) A_c B \int_0^T e^{-w_x t} dt \quad (6)$$

2.2. Fission product removal with spray

The removal of iodine and aerosols from the containment with the spray system can be expressed as depicted in Eqs. (7) and (8), where m_{ri} and m_{ra} are the removal rates of iodine and aerosols, respectively.

$$\frac{dm_{ri,i}(t)}{dt} = P_i(t) - \frac{H\eta_i F}{V} m_{v,i}(t) \quad (7)$$

$$\frac{dm_{ra,i}(t)}{dt} = P_i(t) - \frac{3hFEa}{2dV} m_{v,i}(t) \quad (8)$$

where

$$\eta_i = 1 - e^{-6(K_G \times t_d / d \times (H + K_G / K_L))} \quad (9)$$

and

$$K_G = \frac{D_L}{d} \{2.0 + 0.60 \times \text{Re}^{0.5} \times \text{Sc}^{0.33}\} \quad (10)$$

$$K_L = \frac{2\pi^2 D_L}{3d} \quad (11)$$

$$D_L = \frac{(7.4 \times 10^{-8}) \times \sqrt{(xM_1)} \times T}{\mu_1 v^{0.6}} \quad (12)$$

The values of these parameters in Eqs. (9)–(12) are listed in **Table 3**.

Parameters	Symbols	Values
Partition coefficient	H	200 (for pH 5.0), 5000 (for pH 9.5) and 10,000 ($\text{Na}_2\text{S}_2\text{O}_3$)
Reynolds number	Re	1.29
Schmitt number	Sc	1.742
Molar weights of solvent	Ml (g/mole)	18.01528
Temperature	T (K)	$80 + 273.15$
Molecular volume of I_2	v (cm^3/g)	71.5
Viscosity	μl (centipoise)	0.35
Spray flow rate	F (m^3/sec)	0.35
Degree of solvent	x	2.6 for H_2O

Table 3. Numerical data for spray removal term ([36, 38]).

3. Deterministic computational methodology

Several steps are involved in the simulation of FP behavior inside the reactor building starting from the generation of FP in fuel along with the fuel burn-up. Leakage of FP into the coolant and then from the coolant to containment along with the leakage of coolant. The computational steps are listed in **Figure 3**. A two-stage methodology has

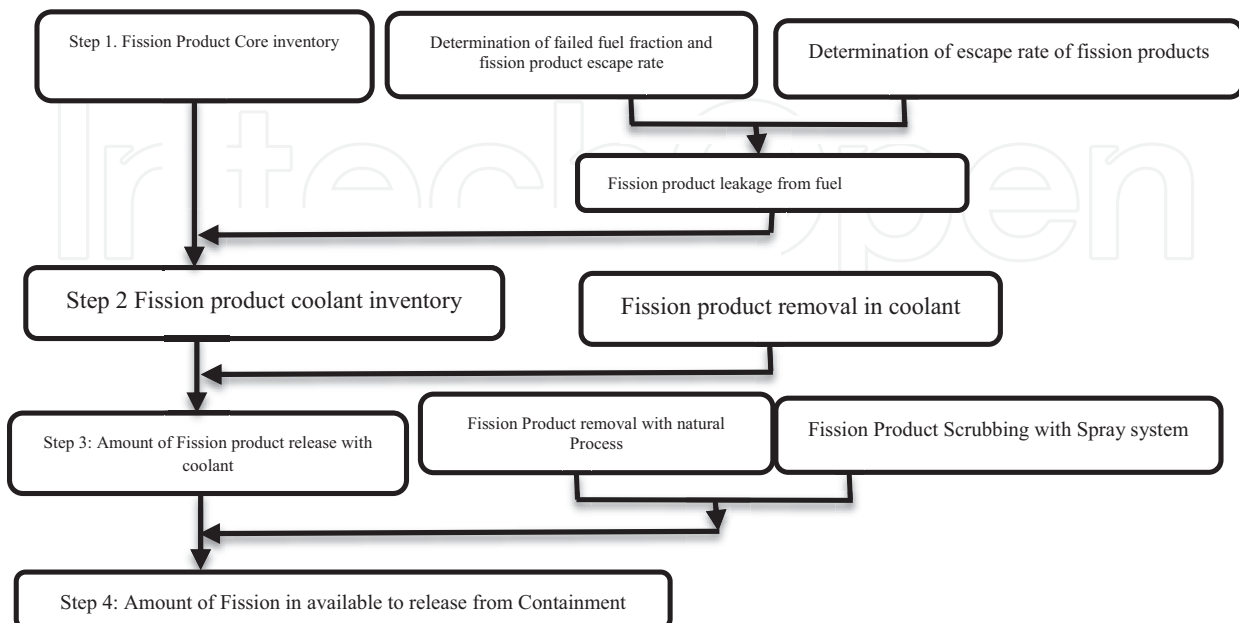


Figure 3. Flow chart of incontinent FP source term estimation.

been adopted: (1) evaluation of activity in the core just before the accident and (2) kinetic quantification of airborne activity under confined conditions. The core activity has been evaluated at for one complete fuel cycle to get maximum core activity. The behavior of airborne FP activity has been quantified for loss of the coolant accident (LOCA) under NUREG-1465 [8] and regulatory guide 1.183 [32] assumptions. The developed model uses subroutine functions containing coupled ODEs and Runge–Kutta (RK) method. The ODEs (Eqs. (1)–(12)) are implemented in MATLAB. The system of ODEs (Eqs. (1), (3), (7), (8)) is coupled and solved numerically using the Runge–Kutta (RK) method in this program.

The RK numerical provides efficient time-domain solution, yielding static as well as dynamic values of FPAs corresponding to about 84 different dominant FPs. The computational cycle starts with the initialization of the variables with $t = 0$. In the time loop, the values of FPAs inside the containment building are calculated using RK scheme for each next time step. The program allows performing these calculations for spray system operation.

4. Implementation in MATLAB

The above equations can be implemented in MATLAB. The flow chart of the MATLAB program is shown in **Figure 4**. In the first step, the physical constant and parameters are defined, and the time array and droplet size are determined by the user.

```
function PWR_Fission_Product
% MATLAB Program for In-containment Fission product program by Khurram Mehboob
% Date : 08-07-2017
%=====
clear; clc; clear all;
%=====
Global Hi Lr V S vd dec r Rr neu EI h Klcm Kgcm d Ea fr H y00 Q y t I Ac D Core_I
Cont_A QQ f x fc B wx YY Sorc wx1
tn = input('Enter end time = tn = '); h = input('Enter stepsize = h = '); t = (0:h:tn); % time array
for d1=100: 100: 1000; % particle diameter (microns)
%=====Control Variables=====
d = d1*1e-4; % particle diameter (cm)
k=d1/100; % Droplet control Factors for printing
fx = 0.20; % activity immediately available in the containment air
fc = 0.35; % core damage fraction.
H =10000; % partition coefficient for iodine
Rr = 4.719; % Recirculation flow rate
Lr = 14.15; % leakage rate
wx = 0.01; % mixing rate
```

In the second step, the fixed variables are loaded from an input text file. The input text file contains the output data from the ORIGEN2.2 code that contains data for 84 different FPs.

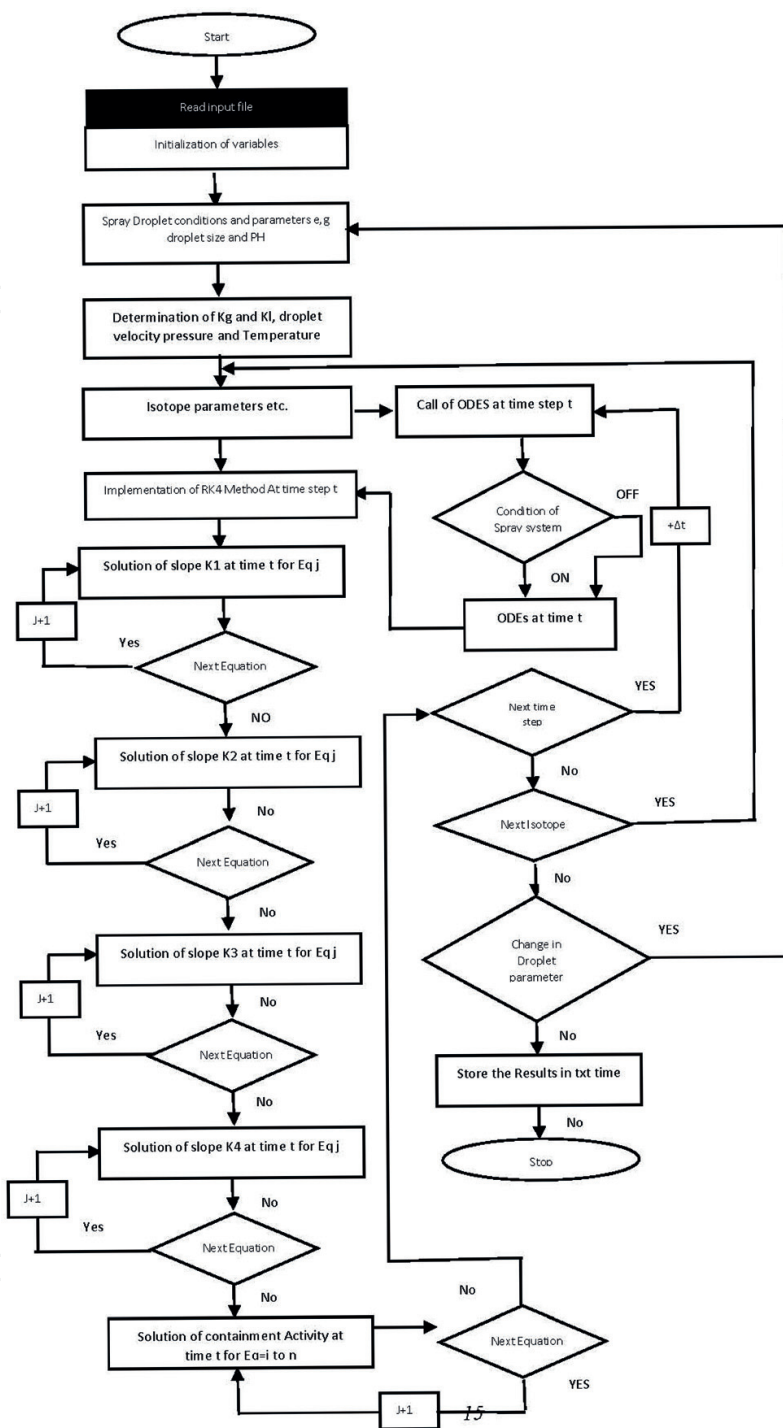


Figure 4. Flow diagram of computer program.

```
load 'input.txt'
%=====Fixed variables=====
V = input2(1,1);           % free volume of the containment
S = input2(2,1);           % free surface of the containment
No_iso = input2(5,1);      % no of isotopes
Hi = input2(6,1);          % height of spray system 40.0 m
fr = input2(10,1);         % Recirculation filtration efficiency
```

```

wx1 = wx/10.0;           % mixing rate of fission products in coolant
K = (wx*wx1)/(wx-wx1);  % normalization constant
%=====
for i = 1:No_iso;       % loop to read isotope data
    Ac = input(i+10,4);  % fission product activity in the core.
    for j = 6:7
        Ac = Ac*input(i+10,j); % Ac*ff*fw
    end
dec = input2(i+10,2);   % decay constant
vd = input2(i+10,08);   % deposition velocity
r = input2(i+10,09);    % resuspension rate
neu = input2(i+10,10);  % heap filter efficiency

```

In the third step, the fixed variables for Eqs. (9)–(12) are solved for droplet by using the data listed in **Table 3**. The values of parameters (T , x , M_l , u_1 , Sc , Re) are the constant variable for the static containment atmosphere.

```

T = 80+273.15;          % Temperature (K)
x = 2.6;                % H2O
Ml = 18.01528;          % molar weight of solvent (g/mole )
v = 71.5;               % molar volume of diffusing substance (l2)
Sc = 1.742;             % Schmidt number.
Re = 1.95;              % Reynold number.
c1 = T-281.615; c2 = (T-281.615)^2; c3 = 8078.4+ c2; c4 = c3^0.5; C = 2.1482*(c1+c4)-120;
ul = (100/C)*2.41908832931* 14.88163900000001; %conversion of Centipoise to g/cm.s

```

Next, the fixed variables are used to determine the dynamics variables (DL , D_{mix} , KG , KL). The Eqs. (9)–(12) are solved using the static data calculated above. Also, the kinetic release of FP is $Q(t)$ that is determined as the function of time.

```

DI2= (((7.4)*(10^-8))*((x*Ml)^0.5)*T)/(ul*(v^0.6)); %diffusion coefficient if I2 (cm2/s)
DIMix = 0.00035*0.258064; %diffusion coeffi of I2 in steam ( cm2/s)
Kgcm = (DIMix/d)*(2.0+0.6*(Re^(1/2))*(Sc^(1/3))); % liquid phase trans coefficient ( cm/s )
Klcm = ((2/3)*(3.1416^2)*(DI2))/(d); % gas phase trans coefficient (cm/s)
vt = ((Re*2387.4)/(d1))^0.508; % terminal velocity (cm/s)
te = (40*100)/(2*vt); % exposure time (s)
A = Kg*(te); BB = d*(H+(Kg/Kl));
EI = (1 - exp(-6*(A/BB))); % FP removal rate (s-1)
Sorcm = Ac*fc/V;
Q = ((1-fx)*B*Sorcm*(exp(-wx1*t)- exp(-wx*t))); % kinetic source

```

Next, the initial conditions for airborne and surface activities are implemented, for example, $m_v(t) = f_x \times f_f \times f_p \times f_c \times A_c/V \text{ g.m}^{-3}$ and $m_s(t) = 0.0$. The kinetic and static parameter values are implemented in coupled equation written as subfunction `diffeq`, and Rang–Kutta fourth-order method is implemented by calling `odeRK4` subroutine function.

%Initial Condition

```
%=====
y00 = fx*fc*Ac/V;   y0 = [y00, 0, 0];
%=====
[t,y] = odeRK4(@diffeq, tn, h, y0);
%=====
YY(:,i)= y(:,1) ;           % YY=y(length(y),:);
I(i)= input2(i+10,1);      % Atoms number
D(i)= input2(i+10,2);      % decay constant
Core_I(i)= input2(i+10,4); % Activity in the core
Cont_A(i)= y00;           % immediate released activity in containment
end
```

The subroutine function containing Eqs. (1), (3), (4) and (7) or (8) is depicted below. The condition for containment spray is controlled in subroutine function here.

```
function dy = diffeq(t,y)
global Lr V S vd dec r F EI H Rr fr fx Ac fc wx B wx1 Q Sorc
if t <=700
    F = 0.0; % input2(8,1); % spray flow rate (0.1-2.0 m3/s)(950 m3/h=0.264m3/s)
else
    F= 0.35;
end
Q = ((1-fx)*B*Sorc*(exp(-wx1*t)- exp(-wx*t)));
dy(1)= -dec*y(1)-(Lr/V)*y(1)-vd*(S/V)*y(1)+r*(S/V)*y(2)-fr*(Rr/V)*y(1)-((F*H*EI)/V)*y(3)+((1-fx)
*B*Ac*(fc/V)*((exp(-wx1*t))-exp(-wx*t)));
dy(2)= vd*y(1)- r*y(2);
dy(3)= Q - ((EI*H*F)/V)*y(3);
end
```

The Range-Kutta fourth-order method is implemented by calling the odeRK4 subroutine function. The function is capable of solving N number of coupled ODEs at separate time steps. The implementation of RK4 method is shown below.

```
% implementation of Range kutta 4thorder method.
function [t,y] = odeRK4(diffeq,tn ,h, y0)
t = (0:h:tn);           % time vector with spacing h
nt = length(t);        % no. of elements in vector t
neq = length(y0);
y = zeros(nt, neq);    % prelocation of y for speed
y(1,:) = y0(:);
h2=h/2;   h3=h/3; h6=h/6;
k1 = zeros(neq,1); k2= k1; k3 = k1; k4= k1; ytemp = k1;
for j=2:nt
```

```

told = t(j-1); yold = y(j-1,:);
k1= feval(diffeq,told, yold);
for n= 1:neq
    ytemp(n) = yold(n) + h2*k1(n);
end
k2= feval(diffeq,told+ h2, ytemp);
for n= 1:neq
    ytemp(n) = yold(n) + h2*k2(n);
end
k3= feval(diffeq,told +h2, ytemp);
for n= 1:neq
    ytemp(n) = yold(n) + h*k3(n);
end
k4= feval(diffeq,told+h, ytemp);
for n= 1:neq
    y(j,n)= yold(n)+h6*(k1(n)+k4(n))+h3*(k2(n)+k3(n));
end
end
end
end

```

5. Some results from numerical simulation

5.1. Volumetric fission product inventory

The core inventory for typical 1000 MW PWR has been evaluated by ORIGEN 2.2 code which is used by our model as a subroutine. A 35% core damage has been considered and 20% (f_x) as the puff release. While the rest of radioactive mass release along with coolant with mixing rate $w_x = 0.01 \text{ s}^{-1}$. The FP release inside the containment building as a function of time is depicted in **Figure 5**. The volumetric radioactive mass found to increase during

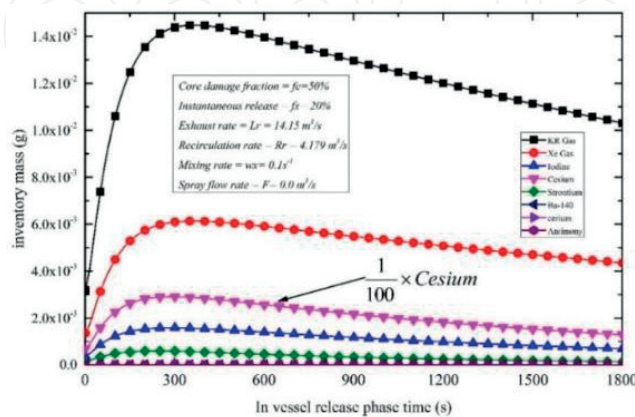


Figure 5. In-containment FP inventory during in-vessel release phase with mixing rate $w_x = 0.01 \text{ s}^{-1}$.

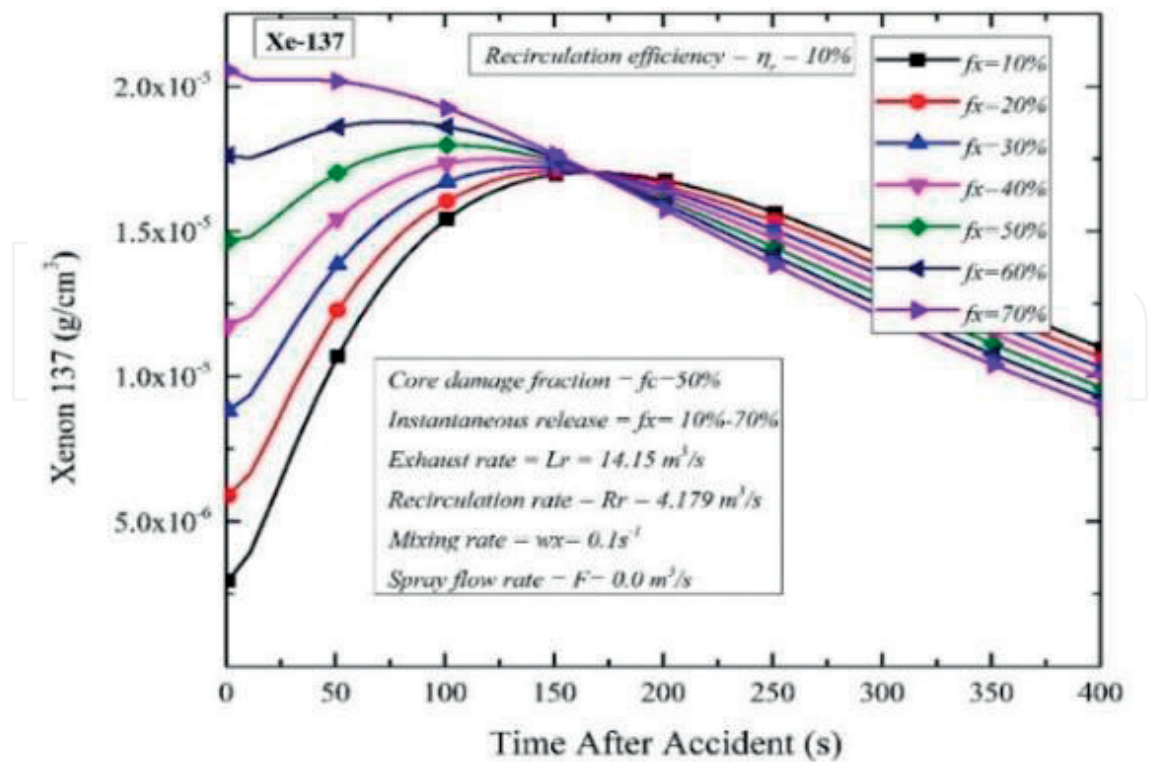


Figure 6. ^{137}Xe activity (g/cm^3) as function of time (s) for various values of f_x and $w_x = 0.01/\text{s}$.

first 300 s then starts decreasing with a constant rate. The cesium found to be dominant with 100 times higher than the other radioactive released masses. The Krypton gas is found to be 15% higher in magnitude with Xenon gas. However, the other isotopes show the similar behavior but with less in magnitude.

5.2. Puff release (f_x) effect on in-containment FPA

The LOCA is due to the uncontrolled leakage from coolant piping (hot leg or cold leg). The coolant burst release generates the immediate escape of radioiodine into containment with the rapture. The volumetric activity of ^{137}Xe inside the containment has been simulated for various values of instantaneous burst release (i.e., $f_x = 10\text{--}70\%$) of total activity inside the core. The simulation results are depicted in **Figure 6**. The results indicated that with the higher percentage of instantaneous release ($f_x = 50\text{--}70\%$), the activity in containment slightly increased and then decreased linearly.

However, a less fraction of burst release ($f_x = 10\text{--}30\%$ of total activity), the activity inside the containment first increases and then starts decreasing after approaching to the maximum value. As the value of f_x decreases, the peak shifts toward higher timescale. The peak becomes more prominent with small values of f_x . This happens due to competition between f_x term in the initial condition and $(1-f_x)(\exp -w_x)$ term in source term (Eq. (4)). The behavior of ^{137}Xe for various values of instantaneous release (f_x) with mixing rate $w_x = 0.01/\text{s}$ explains the clearer picture of airborne Xenon (**Figure 6**).

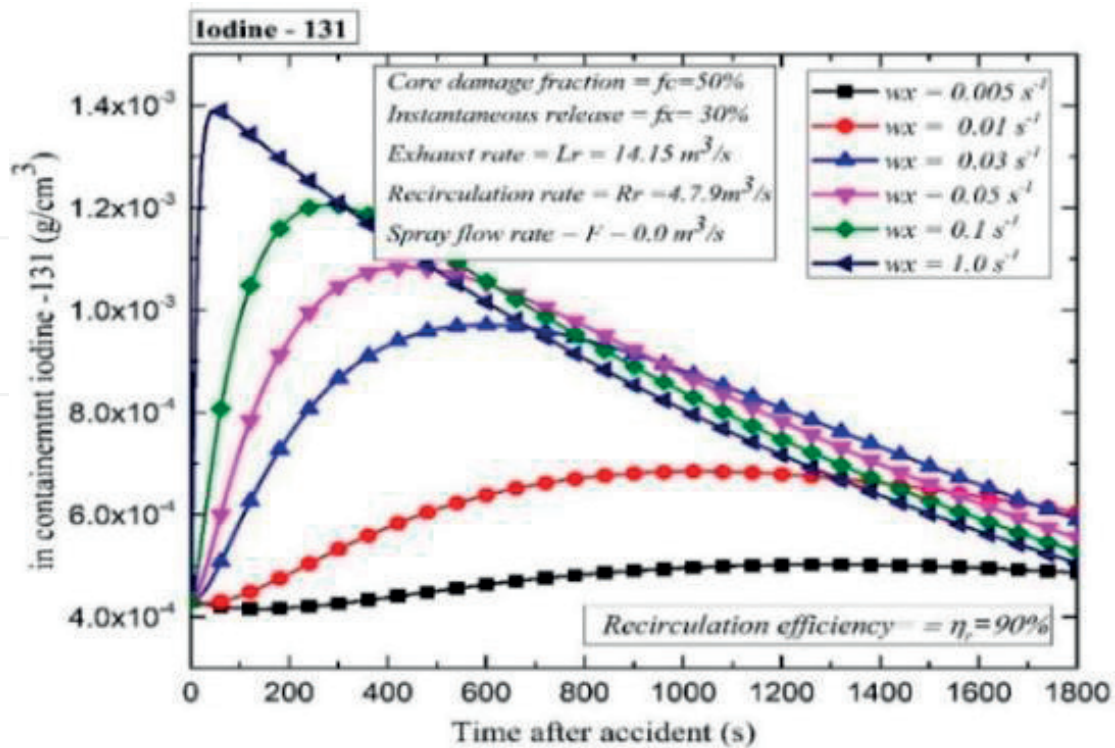


Figure 7. ^{131}I activity (g/cm^3) for ^{131}I as a function of time (s) for various values of w_x .

5.3. Mixing rate (w_x) effect on in-containment FPA

The delayed core released fraction $(1-f_x)(\exp -w_x t)$ for various values of mixing rate w_x which contributes to airborne volumetric activity through coolant has been simulated. The volumetric activity of ^{131}I inside the containment for various values of mixing rate w_x from 0.005 to 1.0 s^{-1} has been numerically simulated. It has been observed that a slight change in the value of w_x results in astonishing variation in airborne activity. The results are shown in Figure 7. For $w_x = 1.0 \text{ s}^{-1}$, highest magnitude has been observed with a shift of peak toward lower timescale value. However, the ^{131}I has been observed to reduce almost linearly with mixing rate 1.0 s^{-1} (Figure 7). The in-containment volumetric concentration of ^{131}I increases and then starts decreasing gradually for mixing rate value from $w_x = 1.0$ to 0.03 s^{-1} ; however, it remains constant for mixing rate 0.005 s^{-1} . This is because of trivial mixing of iodine in the coolant. A higher magnitude of ^{131}I activity has been observed with higher mixing rate.

5.4. Fission product activity with spray system

The primary purpose of the spray system is to mitigate the FP exposure to the environment and to maintain the containment integrity. In this work, we have studied the effect of the spray system in mitigating the radioactive masses (gaseous and particles) released during in-vessel release phase. During loss of coolant accident, the temperature and pressure inside the containment start raising. It reached to 80° pressure and reached to 7.533 psi within few minutes. The simulation has been carried out by assuming the containment temperature at 80°C and pressure at 7.533 psi and the spray with pH 5.0 and 9.5 and the alkaline spray. The spray system is found

to have minimum effect on noble gases and reduces iodine and other radioactive particles effectively. The spray system is started at 100, 500, 1000, and 1500 s after the release time. The effect of spray system activation time on noble gases and iodine is shown in **Figure 8**.

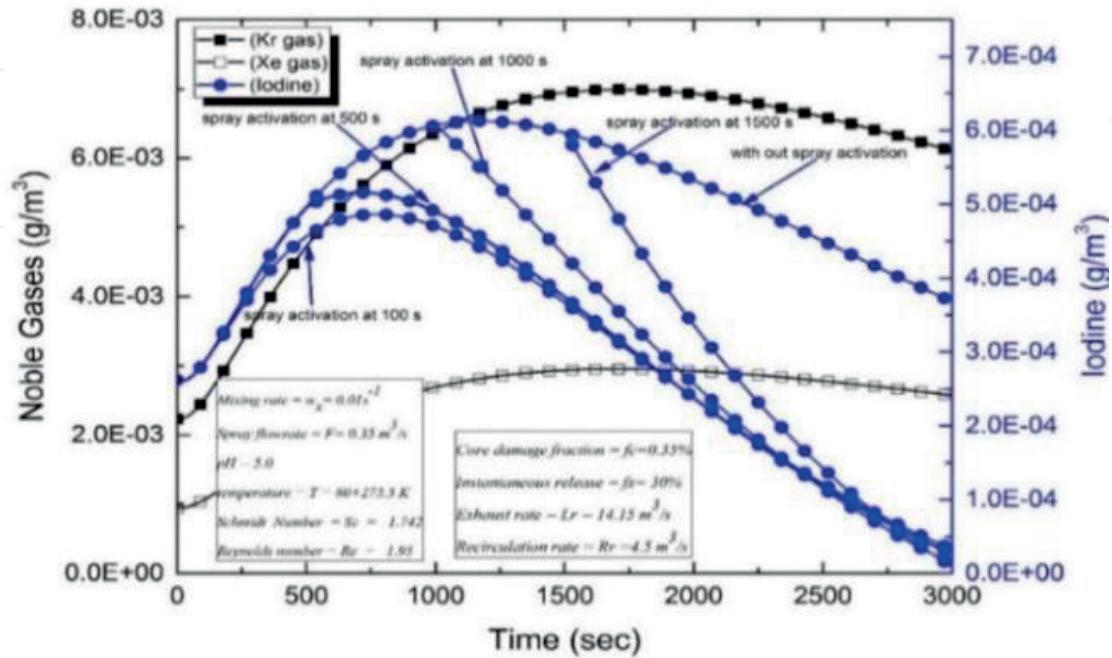


Figure 8. Radioactive noble gases and iodine release during in-vessel release phase with mixing rate $w_x = 0.01 \text{ s}^{-1}$.

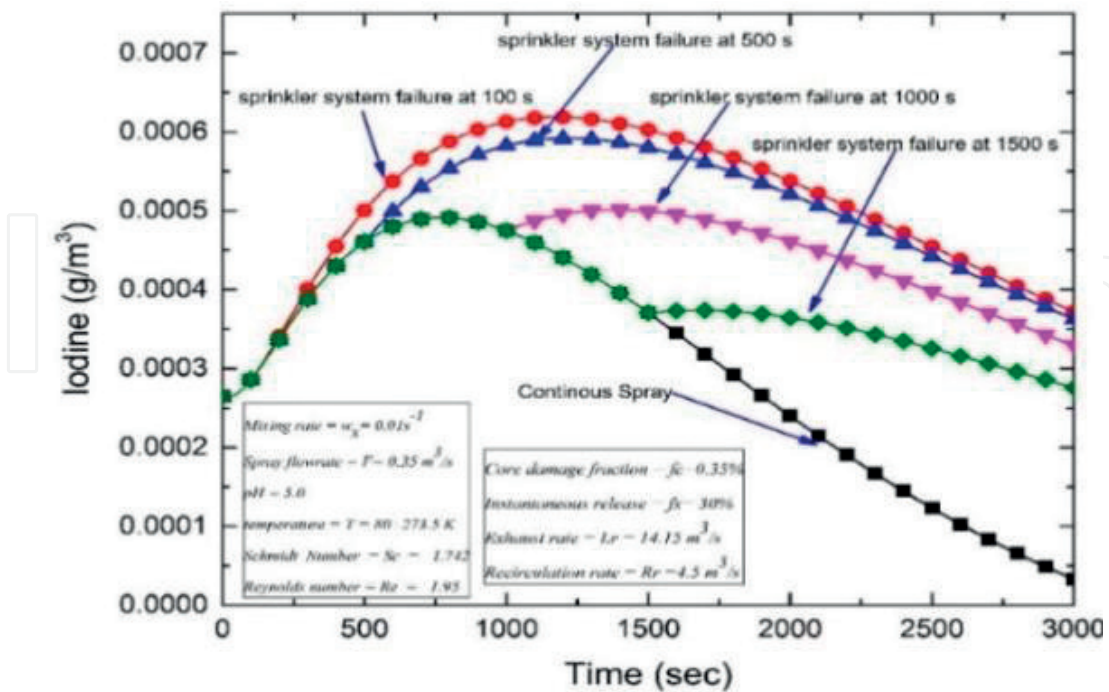


Figure 9. Iodine with containment spray system failures during in-vessel release phase with mixing rate $w_x = 0.01 \text{ s}^{-1}$.

The iodine concentration first increases exponentially in containment and immediately starts reducing with the activation of the spray system. This is because of competition between the continuous source of radioactive iodine (P_i) coming from reactor pressure vessel (RPV) and removal of iodine with the containment spray system (**Figure 8**). The volumetric iodine starts reducing exponentially after the activation of the spray system. The droplet size has been assumed 800 microns for the simulation. However, the noble gases are observed to be unaffected with a spray system. The response of airborne iodine to the failure of the spray system is depicted in **Figure 9**.

Figure 9 indicates that the premature failure of the system ($t = 100$ s) does not affect the airborne iodine concentration. The slight decrease in airborne iodine concentration is seen if the spray system is failed or malfunctions at 500 s. However, the spiracles are operated for a longer period, for example, 1000–1500 s during the in-vessel phase. The airborne concentration of iodine is reduced significantly. The failure of the system at 1000 and 15,000 s caused the regaining of airborne iodine (**Figure 9**).

5.5. Droplet diameter and pH effect on in-containment FPA

The droplet collection efficiency of spray also depends on the containment atmospheric temperature, pressure and spiracle pH value. The effect of spray water pH value and an alkaline spray has been simulated. The results are depicted in **Figure 10**. The results showed that the higher pH spray solution (pH 9.5) and alkaline solution ($\text{Na}_2\text{S}_2\text{O}_3$) have similar removal characteristics for airborne iodine. The iodine removal rates of Boric (pH 5.0), NaOH (pH 9.5) and alkaline solution with different droplet sizes are shown in **Figure 11**.

The removal rate has been seen to decrease exponentially with the increase in droplet size for an alkaline solution (**Figure 11**). However, for a spray solution with pH value 5.0, the removal rate decreases in a linear manner. The in-containment volumetric mass under the atmospheric

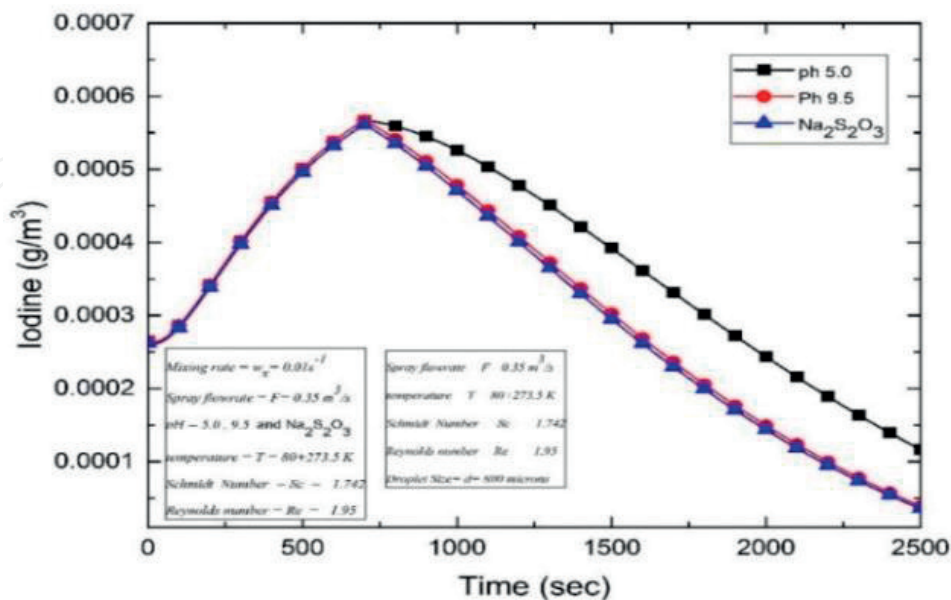


Figure 10. Response of radioactive iodine for spray pH value during in-vessel release phase with mixing rate $\omega_x = 0.01 \text{ s}^{-1}$.

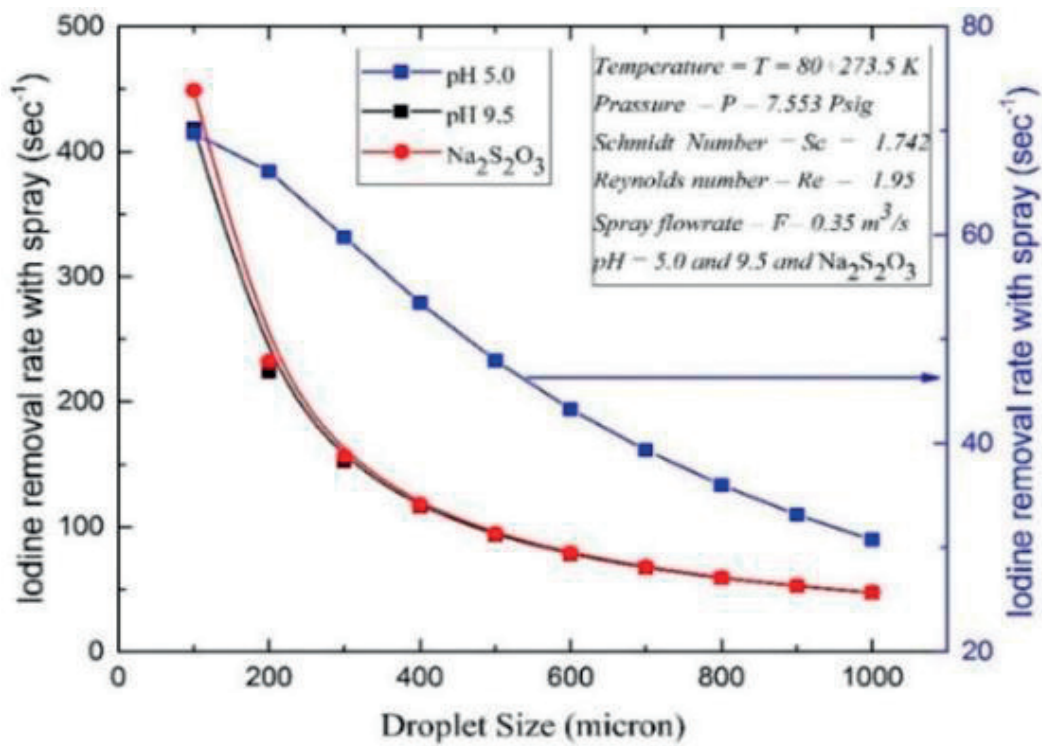


Figure 11. Droplet removal rate for iodine at pH 5.0, 9.5 and with alkaline spray solution ($\text{Na}_2\text{S}_2\text{O}_3$).

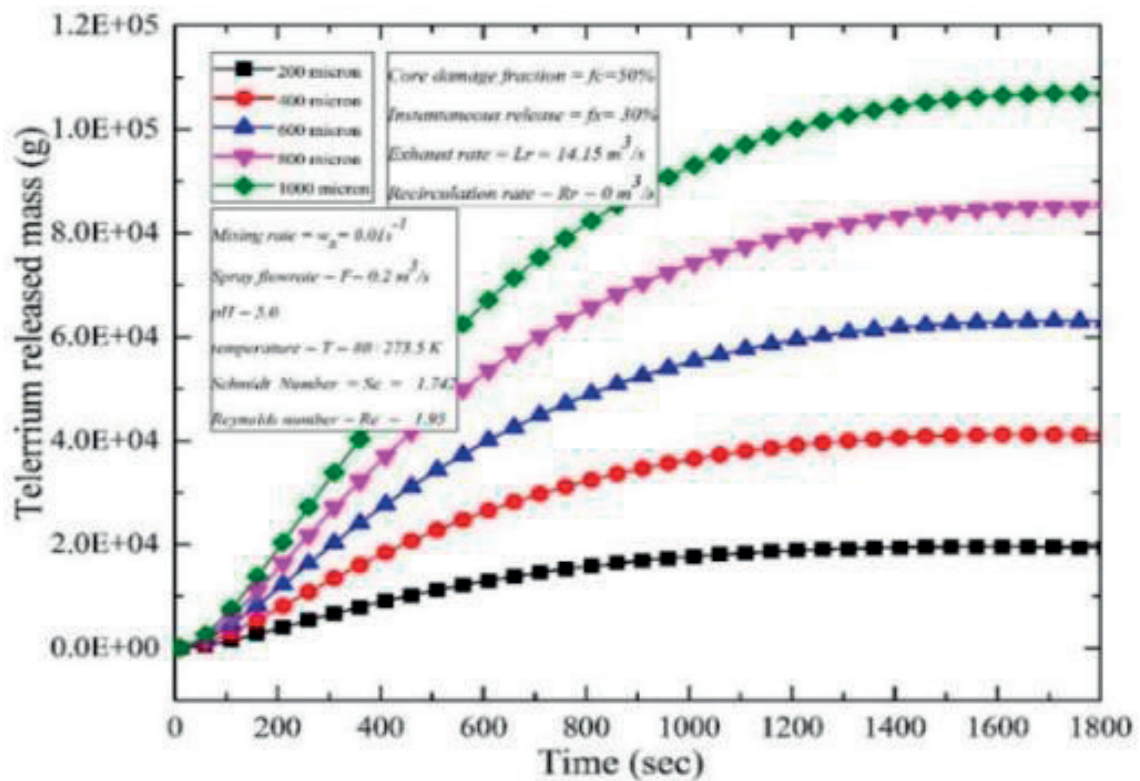


Figure 12. Tellurium inventory during in-vessel release phase with mixing rate $\omega_x = 0.01 \text{ s}^{-1}$.

conditions with a temperature of 80°C and 7.533 Psi. Assuming 35% core damage and 20% burst release. The rest of mass is assumed to release along with the coolant with mixing rate $w_x = 0.01 \text{ s}^{-1}$. The mass concentration of tellurium is simulated for droplet sizes (100–1000 microns). The containment spray system is activated with the initiation of an accident with a constant flow rate of $0.2 \text{ m}^3/\text{s}$.

Simulation results showed that the droplet size is quite effective to reduce the airborne FPs. It has been observed that the concentration of airborne tellurium decreases with a decrease in droplet size (**Figure 12**). The peak concentration in Tellurium mass reaches to a maximum concentration at a longer time with the higher droplet diameter. The magnitude of maximum concentration has been found the approximately inverse square of droplet diameter ($1/d^2$). The containment spray system removal rate for iodine versus droplet diameter is depicted in **Figure 11**. The maximum removal rate has been found 452 s^{-1} with alkaline solution spray with a droplet size of 100 micrometers. The removal rate is found to decrease exponentially as the droplet diameter increases. 44.7 s^{-1} removal rate has been seen for 1000-micron diameter droplet size for pH 9.5 and alkaline spray solution with spray flow rate $0.35 \text{ m}^3/\text{s}$. The gas phase and liquid phase coefficients play a vital role in absorption efficiency. Both gas- and liquid-phase mass transfer coefficients (K_G and K_L) decrease drastically with an increase in droplet size (**Figure 13**). However, the gas- and liquid-phase mass transfer coefficients (K_G and K_L) are also related to the inverse square of droplet diameter ($1/d^2$).

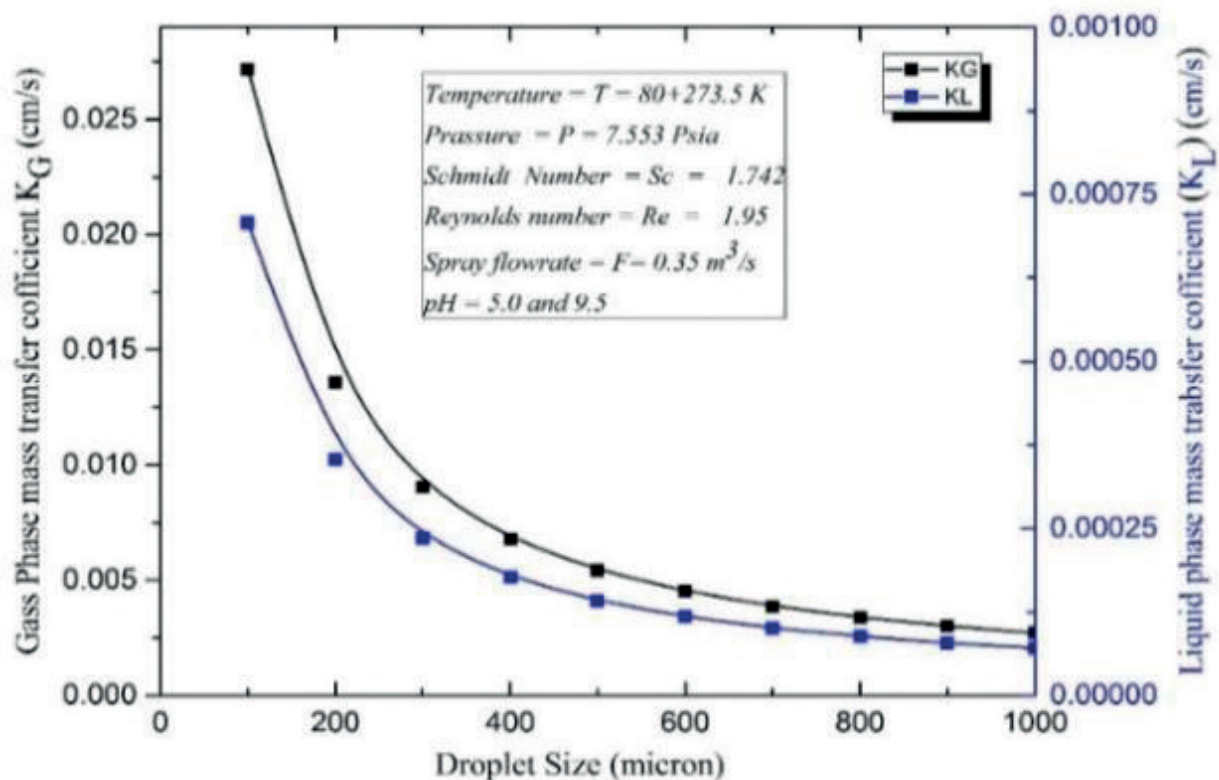


Figure 13. A comparison of gas-phase mass transfer coefficient (K_G) and liquid-phase mass transfer coefficients (K_L) for elemental iodine constant pH = 5.0, T = 80°C.

6. Conclusion

This chapter has presented the numerical simulation of FP activity inside the reactor containment building under LOCA. The numerical simulation of in-containment FPs against the mixing rate, puff release, droplet diameter, spray pH value and spray performance has been simulated. The results indicate that the mixing rate of FPs in coolant significantly affects airborne FP activity inside the containment. The higher pH spray solution (9.5) and spray with sodium thiosulfate ($\text{Na}_2\text{S}_2\text{O}_3$) have observed similar scrubbing properties. The droplet size is significantly important for removal of FP. There is a higher tendency of FP to interact with airborne particles (**Figure 11**) with, due to their higher values of liquid- and gas-phase mass transfer coefficients (K_L and K_G) (**Figure 13**). Therefore, the acceptance criteria of droplet size have been suggested between 600 and 800 microns, with pH value higher than 7.0 which delivers higher removal rate. The earlier the containment spray system has operated, the airborne concentration will be minimum (**Figure 8**). However, the delay operation caused the higher airborne concentration of radioactive mass. It has also been observed if the containment spray system is failed during in-vessel phase a regain will be caused in radioactive mass (**Figure 9**). Based on our work, we are suggesting 600–8500 microns mean droplet diameter containment spray system should be used to get maximum radiation hazard safety. Moreover, from our results, we can conclude that the spray system should be operated within 500 s after the accident and should be operated more than 3000 s (whole in vessel phase). The uncertainties in simulated results depend on generally available data in the literature.

Acknowledgements

This article was funded by the deanship of scientific research (DSR) at King Abdul Aziz University, Jeddah. The author, therefore, acknowledges with thanks DSR for technical and financial support.

Author details

Khurram Mehboob* and Mohammad Subian Aljohani

*Address all correspondence to: khurramhrbeu@gmail.com

Department of Nuclear Engineering, Faculty of Engineering, King Abdul Aziz University, (KAU), Jeddah, Saudi Arabia

References

- [1] Rahim FC, Rahgoshay M, Mousavian SK. A study of large break LOCA in the AP1000 reactor containment. *Progress in Nuclear Energy*. 2012;**54**:132-137

- [2] Huang GF, et al. Study on mitigation of in-vessel release of fission products in severe accidents of PWR. *Nuclear Engineering and Design*. 2010;**240**(11):3888-3897
- [3] Denning RS, et al. Radionuclide Release Calculations for Selected Severe Accident Scenarios. NRC NUREG/CR-4624, 1986
- [4] Lewis BJ, et al. Fission product release mechanisms during reactor accident conditions. *Journal of Nuclear Materials*. 1999;**270**:21-38
- [5] Iglesias FC, et al. Fission product release mechanisms during reactor accident conditions. *Journal of Nuclear Materials*. 1999;**270**:21-38
- [6] Mehboob K, et al. Source term evaluation of two loop PWR under hypothetical severe accidents. *Annals of Nuclear Engineering*. 2012;**50**:271-284
- [7] Tigras A, Bachet M, Catalette H, Simoni E. PWR iodine speciation and behavior under normal primary coolant conditions: An analysis of thermodynamic calculations, sensibility evaluations and NPP feedback. *Progress in Nuclear Energy*. 2011;**53**:504-515
- [8] Soffer L, et al. Accident Source Terms for Light-Water Nuclear Power Plants. NUREG-1465, U.S. Nuclear Regulatory Commission 1995
- [9] Dehjourian M, et al. Effect of spray system on fission product distribution in containment during a severe accident in a two-loop pressurized water reactor. *Nuclear Engineering and Technology*. 2016;**48**:975-981
- [10] Rosen M, Jankowski M. Reassessing releases: A closer look at source term. IAEA Bulletin. Special Report. 1985:43-46
- [11] Ducros G, et al. Fission product release under severe accidental conditions general presentation of the program and synthesis of VERCORS 1-6 results. *Nuclear Engineering and Design*. 2001;**20**(2):191-203
- [12] Lewis BJ, et al. Overview of experimental programs on core melt progression and fission product release behaviour. *Journal of Nuclear Materials*. 2008;**380**(1-3):126-143
- [13] Luis E, Herranz B. Clement in-containment source term key insights gained from a comparison between the PHEBUS-FP programme and the US-NRC NUREG-1465 revised source term. *Progress in Nuclear Energy*. 2010;**52**(5):481-486
- [14] Giraulta N, et al. LWR severe accident simulation: Iodine behavior in FPT2 experiment and advances on containment iodine chemistry. *Nuclear Engineering and Design*. 2012;**243**:371-392
- [15] Hastet T, et al. Phébus FPT3: Overview of main results concerning the behaviour of fission products and structural materials in the containment. *Nuclear Engineering and Design*. 2013;**261**:333-345
- [16] Mäkynen JM, et al. Experimental studies on hygroscopic aerosol behaviour in LWR containment conditions. *Journal of Aerosol Science*. 1994;**25**(Suppl. 1):247-248

- [17] Mäkynen JM, et al. AHMED experiments on hygroscopic and inert aerosol behaviour in LWR containment conditions: Experimental results. *Nuclear Engineering and Design*. 1997;**178**(1-2):45-59
- [18] Schwarz M, et al. PHEBUS FP: A severe accident research programme for current and advanced light water reactors. *Nuclear Engineering and Design*. 1999;**187**:47-69
- [19] Girault N, et al. Towards a better understanding of iodine chemistry in RCS of nuclear reactors. The 2nd European Review Meeting on Severe Accident Research (ERMSAR-2007) Forschungszentrum Karlsruhe GmbH (FZK), Germany, 12–14 June 2007
- [20] Di Giuli M, et al. SARNET benchmark on Phébus FPT3 integral experiment on core degradation and fission product behaviour. *Annals of Nuclear Energy*. 2016;**93**:65-82
- [21] Kljenak, et al. Thermal-hydraulic and aerosol containment phenomena modelling in ASTEC severe accident computer code. *Nuclear Engineering and Design*. 2010;**240**(3):656-667
- [22] Haste T, et al. MELCOR/MACCS simulation of the TMI-2 severe accident and initial recovery phases, off-site fission product release and consequences. *Nuclear Engineering and Design*. 2006;**236**(10):1099-1112
- [23] Slaga AC, et al. MAAP4.0.7 severe accident source term analysis, In Proceedings of the International Congress on Advances in Nuclear Power Plants (ICAPP ' 08), 2008. Anaheim, Calif, USA, Paper 8201
- [24] Singh M, et al. A numerical methodology for estimation of volatile fission products release from nuclear fuel. *Nuclear Engineering and Design*. 2017;(323):338-344
- [25] Lewis BJ, et al. Fission product release modelling for application of fuel-failure monitoring and detection - an overview. *Journal of Nuclear Materials*. 2017;**489**:64-83
- [26] Lewis BJ. A generalized model for fission product transport in the fuel-to-sheath gap of defective fuel elements. *Journal of Nuclear Materials*. 1990;**175**(3):218-226
- [27] Koo YH, Sohn DS, Yoon YK. Release of unstable fission products from defective fuel rods to the coolant of a PWR. *Journal of Nuclear Materials*. 1994;**209**(3):248-258
- [28] Avinov AS. The model of the fission gas release out of porous fuel. *Ann.Nucl. Eney*. 1998;**25**(15):1275-1280
- [29] Tucker MO, White RJ. The release of fission products from UO₂ during irradiation. *Journal of Nuclear Materials*. 1979;**87**(1):1-10
- [30] Awan SE, et al. Sensitivity analysis of fission product activity in primary coolant of typical PWRs. *Progress in Nuclear Energy*. 2011;**53**(3):245-249
- [31] Javed Iqbal M, et al. Kinetic simulation of fission product activity in primary coolant of typical PWRs under power perturbations. *Nuclear Engineering and Design*. 2007;**237**(2):199-205
- [32] USNRC. Alternative Radiological Source Terms for Evaluating Design Basis Accidents at Nuclear Power Reactors, Regulatory Guide 12000. p. 183

- [33] USNRC, Reactor Safety Study. An Assessment of Accident Risk in U.S. Commercial Nuclear Power Plants, WASH-1400, United States Nuclear Regulatory Commission 1975
- [34] Henry RE, TMI-2: A Text Book in Severe Accident Management, MISD Professional Development Workshop, ANS/ENS international meeting, 2007
- [35] Jak K. Nuclear Power Plant Modelng and Steam Generator Stability Analysis. PhD Thsis. The University of Michigan; 1981
- [36] Mehboob K, et al. Numerical simulation of radioisotope's dependency on containment performance for large dry PWR containment under severe accidents. Nuclear Engineering and Design. 2013;**262**:435-445
- [37] El-Jaby, et al. A general model for predicting coolant activity behavior for fuel failure monitoring analysis. Journal of Nuclear Materials. 2010;**399**:87-100
- [38] Mehboob K, Aljohani SM. Modeling and simulation of radio-iodine released inside the containment as result of an accident. Progress in Nuclear Energy. 2016;**88**:75-87